



IN-20-TIR
© DOWNRIDE

7980
9-12

NASA-TM-111264

AIAA 95-2590

**Plume Particle Collection and Sizing From
Static Firing of Solid Rocket Motors**

J.K.Sambamurthi
NASA/Marshall Space Flight Center
Huntsville, Alabama

**31st AIAA/ASME/SAE/ASEE
Joint Propulsion Conference and Exhibit
July 10-12, 1995/San Diego, CA**

For permission to copy or republish, contact the American Institute of Aeronautics and Astronautics
370 L'Enfant Promenade, S.W., Washington, D.C. 20024

PLUME PARTICLE COLLECTION AND SIZING FROM STATIC FIRING OF SOLID ROCKET MOTORS

Jay K. Sambamurthi*
NASA Marshall Space Flight Center
Huntsville, Alabama

Abstract

A unique dart system has been designed and built at the NASA Marshall Space Flight Center to collect aluminum oxide plume particles from the plumes of large scale solid rocket motors, such as the space shuttle RSRM. The capability of this system to collect clean samples from both the vertically fired MNASA (18.3% scaled version of the RSRM) motors and the horizontally fired RSRM motor has been demonstrated.

The particle mass averaged diameters, d_{43} , measured from the samples for the different motors, ranged from 8 to 11 μm and were independent of the dart collection surface and the motor burn time. The measured results agreed well with those calculated using the industry standard Hermesen's correlation within the standard deviation of the correlation. For each of the samples analyzed from both MNASA and RSRM motors, the distribution of the cumulative mass fraction of the plume oxide particles as a function of the particle diameter was best described by a monomodal log-normal distribution with a standard deviation of 0.13 - 0.15. This distribution agreed well with the theoretical prediction by Salita using the OD3P code for the RSRM motor at the nozzle exit plane.

Introduction

Thermal radiation from the plume of any solid rocket motor containing aluminum as one of the propellant ingredients, is mainly from the 0.1 to 20 μm hot aluminum oxide (Al_2O_3) particles in the plume. The plume radiation to the base components of a flight vehicle is primarily determined by the plume flowfield properties, the size distribution of the plume particles,

* Aerospace Engineer, Senior Member AIAA

Copyright © 1995 by the American Institute of Aeronautics and Astronautics, Inc. No copyright asserted in the United States under Title 17, U.S. Code. The U.S. Government has a royalty-free license to exercise all rights under the copyright claimed herein for government purposes. All other rights are reserved by the copyright owner.

and their optical properties. The optimum design of a vehicle base thermal protection system (TPS) is dependent on the ability to predict accurately this intense thermal radiation using validated theoretical models.

Currently, the design thermal radiation to the base region of the shuttle components from the Redesigned Solid Rocket Motor (RSRM) plumes is predicted using a simple empirical model¹ based on flight measured data. However, a more advanced reverse monte-carlo method² has been developed recently for the Advanced Solid Rocket Motor (ASRM) program. This model is currently being validated using measured radiation data from flight motors as well as static firing of the full-scale motors at the Thiokol Space Operations Facility in Utah and the 18.3% scaled modified NASA (MNASA) motors at NASA / Marshall Space Flight Center (MSFC). Such validations enable one to gain confidence in the monte-carlo model. Application of this model to the RSRM design thermal radiation environments is expected to improve the current design environments and to reduce the TPS requirements in the base region of the shuttle.

One of the major unknowns in the inputs to the theoretical monte-carlo radiation model is the size distribution of the Al_2O_3 particles in the plume. In the absence of any experimental results for the plume particle size distribution from a full-scale RSRM, a theoretical distribution³ was used in the model consisting of five equal mass fractions based on a normal distribution about a mass averaged diameter, d_{43} . Radiation predictions made on such a theoretical particle size distribution tend to be conservative when compared with measured data. Such conservatism will be reduced if the actual particle size distribution in the plume is used.

Plume particle size characterization efforts have been conducted in the past for motors of different sizes, and an excellent summary has been presented by Hermesen⁴. However, these analyses have been primarily to predict a mass averaged diameter, d_{43} , in the nozzle to accurately account for the two phase flow losses in the motor performance calculation, and did not include any full-scale motors of the RSRM size.

Salita⁵ has summarized the recent attempts to measure Al_2O_3 particle size in solid rocket motor chambers, nozzles, and plumes. Six of the 19 studies he summarized related to collection of plume particles from solid rocket motors, varying in size from very small micromotors to large Titan motors. The plume particle size distribution varied widely among these different studies and were strongly dependent on the particle collection methods. Also, Salita⁶ employing a corrected version of the One-Dimensional 3-Phase (OD3P) code and an improved model of particle collision/coalescence in the nozzle flow has predicted a log normal monomodal particle size distribution for the full scale RSRM motor at the nozzle exit plane.

Girata, et al.,⁷ have sampled plume particles from small motors to determine the harmful effects of the plume on the mission. Here the samples were collected by a probe placed 8 feet downstream of the nozzle exit plane. There were no differences in the samples obtained at the edge or centerline of the plume. However, the absence of the large particles in the samples seemed to indicate that only the smoke particles were collected by the probes. To study the impact of Titan launches on the environment, Strand, et al.,⁸ sampled the plume particle filled atmosphere immediately after Titan launches. However, these particle collection systems were not located in the plume during the actual firing of the motor. They collected samples 7-23 minutes after the passage of the vehicle by flying through the plume trail in a helicopter and a U-2 plane. The large particles might have settled long before the actual collection of the particles. Kohlbeck, et al.,⁹ have collected plume particles from several large motors and observed Al_2O_3 particles in the 0.5 to 8 μm range. Laredo, et al.,¹⁰ investigated the oxide particle size inside and in the plume of micromotors (0.5 cm throat diameter) with RSRM propellant. Salita's analysis of Laredo's results⁵ indicated that the measured d_{43} was twice that of Hermesen's prediction. Also, 53% of the plume particle mass was smaller than 2 μm in contrast to the prediction of 1-2% by Salita⁶. After further studies with these micromotors, Gomes, et al.,¹¹ determined that the presence of large particles in the plume was a function of the periodic accumulation and shedding of large agglomerates due to the very small nozzle throat diameters. Several firings of these micromotors may be required to resolve the differences between the experimental observations and the theoretical predictions by Salita.

All the plume particle collection techniques described above have been successful in collecting either

only submicron particles^{7,8} or larger particles⁹ but not both sizes with the same technique. However, both sizes do exist in the plume and analytical model such as OD3P support their coexistence. The results from each of the above experimental techniques were probably dependent on the biases of their experimental procedures.

This article describes a successful effort to collect reasonably clean plume particle samples from the static firing of large solid rocket motors, and to measure the d_{43} and the size distribution of the Al_2O_3 particles from these samples. The motors investigated included the RSRM designated as Flight Support Motor No. 4 (FSM-4) test fired at the T-24 test stand at the Thiokol space operations facility in Utah, as well as three 18.3% scaled MNASA motors (MNASA 8-10) tested at NASA/MSFC. Prior attempts to collect plume particles from full-scale motor firings have been unsuccessful due to the extremely hostile thermal and acoustic environment in the vicinity of the motor nozzle.

Particle Collection Method

A plumbing schematic of the plume particle collection system is presented in Figure 1. The principle behind this particle collection technique is to pneumatically launch darts through the plume during the motor firing and collect the plume particle samples on sticky copper tapes mounted at different locations on the dart.

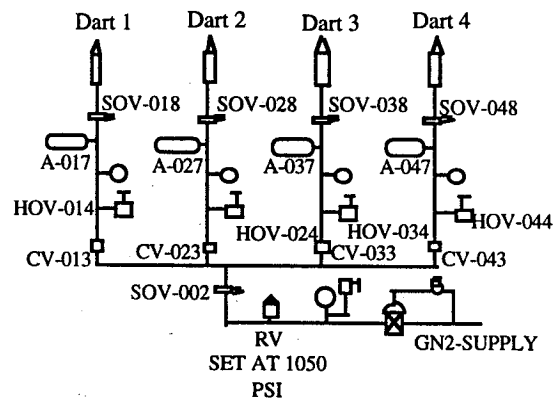


Figure 1. High Pressure Plumbing Schematic for the Dart System.

The pneumatic system consisted of a launcher with a bank of four accumulators (A-017 through A-047) and an electronic control box. Each accumulator was connected through a check valve (CV-013 through

CV-043) to a common high pressure nitrogen source and a solenoid valve as shown in Figure 1. Also, each accumulator was connected to a launch tube through a high flow rate valve activated by a solenoid. These four valves and solenoids are indicated as SOV-018, 028, 038, and 048 in Figure 1. To prepare for launching, individual darts were inserted over each launch tube, the solenoid valves were closed by the control box to ensure no leakage of high pressure gas into the launch tube, and the accumulators were loaded with high pressure nitrogen to 800 psi. The darts were launched individually by opening the high flow rate valves using the solenoids triggered by a time sequencer in the control box. The control box time sequencer was initiated by the motor firing sequencer at ignition. Each accumulator was also provided with a safety hand valve (HOV 014 - 044) for bleeding the accumulator in the event of a misfire or delay in the static test.

MNASA Method

A simple 40-inch long projectile weighing about 13 lbs (Figure 2) was utilized in the MNASA tests. The Al₂O₃ plume particles were collected by sticky copper tapes affixed at different locations on the shaft and fins of the dart. Stainless steel wires of diameters varying from 1/4-inch to 1/32-inch were welded around the dart. Sticky copper tapes were affixed to these wires also to collect the plume particles. Any possible biasing in the size distribution of the particles collected by the main shaft of the dart can be examined by studying the particles gathered by these wires.

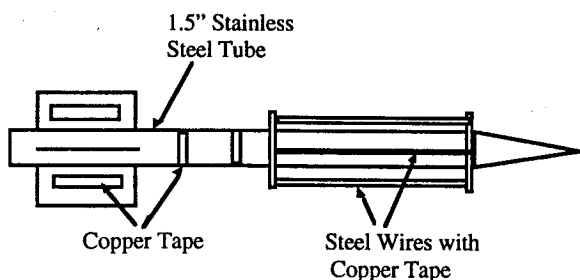


Figure 2. Projectile Launched Through the Plume in the MNASA Tests

The MNASA motors were tested vertically upward with the exit plane of the nozzle located about 30 ft above the ground. The general characteristics of the motors, MNASA 8-10, are given in Table 1. The launcher was located 55 feet from the motor centerline. The projectiles were launched at 80° measured from the horizontal. The projectile had an approximate launch velocity of 125 ft/sec. It was estimated to enter the

plume at about 150 feet from the nozzle exit plane and exit at about 620 feet. The residence time in the plume was estimated to be about 5 seconds. The projectiles landed nose first and buried about 1.5 ft into the ground. The launcher had a single dart capability for the MNASA 8 test, but was capable of launching five projectiles for MNASA 9 and 10 tests. In MNASA 8 test, one projectile was launched 1 second after motor ignition; in MNASA 9 test, five projectiles were launched at 1, 3, 5, 7, and 15 seconds after ignition; and in MNASA 10 test, five projectiles were launched at 1,3,5,7, and 9 seconds after ignition. All the projectiles were successful in collecting particles from the plume. Projectiles 3 and 4 of MNASA 10 test did not land nose forward. Hence, the samples were severely contaminated and not included in the size distribution analysis.

	MNASA 8	MNASA 9	MNASA10
Nozzle	Contour	Conical	Conical
Throat D (in)	9.986	9.958	9.958
Exp. Ratio	7.583	5.5587	5.5587
Propellant	ASRM	RSRM	RSRM
% Aluminum	19	16	16
Ch.Pressure	624	717	650

Table 1. Some General Characteristics of the MNASA Motor Tests Where Plume Particles Were Sampled.

RSRM Method

The full-scale RSRM static test motor is fired horizontally. The motor centerline is about 10 feet above ground level and the motor is fired into a hill about 800 feet aft of the nozzle exit plane.

For the FSM-4 test, the dart system was located 285 feet aft of the nozzle exit plane and about 200 feet from the motor centerline. The launch angles of the darts were such that they were aimed about 10 - 20 feet below the upper boundary of the plume along the plume centerline. The plume diameter at 285 feet aft of the nozzle is estimated to be about 90 feet. The aim point of the darts was dictated by the need for the dart to survive the high dynamic pressure of the plume. The dynamic pressure is considerably reduced near the outer boundary of the plume. This improved the survivability of the dart. Moreover, the higher launch angle of the dart increased the range of the dart's trajectory and protected the dart from the hostile exhaust environment after its traverse through the plume. The plume height also minimized the contamination by dust and dirt picked up from the ground by the motor plume.

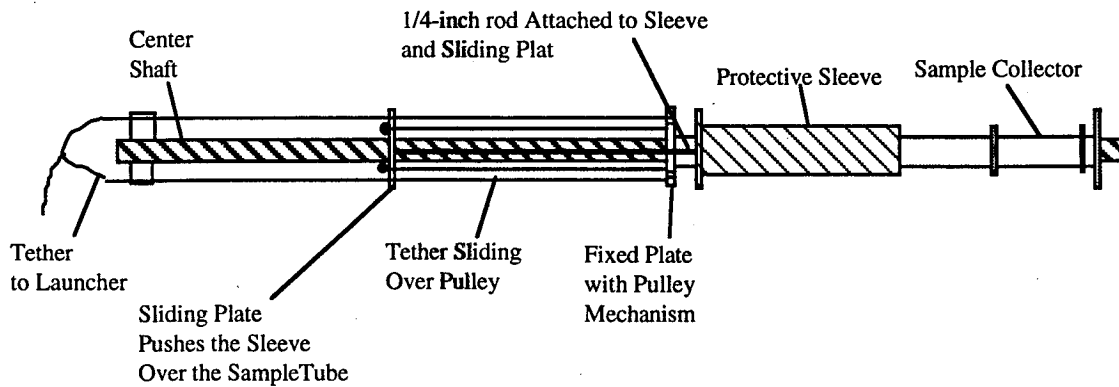


Figure 3. Tethered Dart Employed in the FSM-4 Test To Collect Reasonably Clean Plume Samples

Two different types of darts were launched in the FSM-4 test. One of them was a control dart weighing about 6 lbs and was basically a scaled version of the dart (Figure 2) employed in the MNASA program. It was employed here due to its success in collecting plume samples from the MNASA motor. However, due to the orientation of the RSRM motor during the static test, a large recirculating cloud of dust and dirt is created as the plume impacts the hill aft of the nozzle. Consequently, a new dart design was needed to keep the plume particle sample contaminant free until the darts could be retrieved.

The new dart designed for the full-scale test to minimize the contamination of the samples is shown in Figure 3. The plume particle samples were collected on copper tapes affixed to a 1.5 inch diameter stainless steel tube over a 10-inch long area. A cylindrical sleeve, activated by a plate-pulley mechanism and attached to a 240 feet long tether, slid over the sample area to protect the sample after it was collected in the plume. The sleeve was also designed with a positive latch mechanism to prevent opening of the sleeve upon ground impact. Both the 1.5-inch sample tube and the cylindrical sleeve were inserted over a 48-inch long aluminum shaft. The tether was a 1/16-inch diameter steel wire wound around an inverted canister. The tail end of the tether was attached to a hook on the launcher and the head end to the plate/pulley mechanism on the dart. When the end of the tether was reached during the flight of the dart, the tether pulled the cylindrical sleeve over the sample area and disengaged the sample collecting tube with the sleeve from the center aluminum shaft. The sample with its protective shield

followed a ballistic path and safely landed on the other side of the plume. The aluminum shaft stayed attached to the tether and was destroyed by the plume. The length of the tether was selected such that the sleeve was engaged over the sample area when the dart was just about to leave the plume.

Individual protective housings were also built over the darts on the launcher to protect the darts from contamination between motor ignition and dart launch.

In the FSM-4 test, the tethered darts were launched at 12.3, 67.0, and 93.5 seconds and the control dart was launched at 68.3 seconds after motor ignition. All four darts were launched during three separate nozzle pitch-up events which elevated the plume by about 25 feet at 300 feet aft of the nozzle exit plane. This further ensured the ability of the darts to collect relatively clean samples from the plume. The residence time of the darts in the plume was estimated to be about 0.5 seconds. Both dart designs weighed about 6 lbs.

The two tethered darts launched at 12.3 sec and 93.5 sec and the control dart launched at 68.3 sec functioned nominally. The range of the darts was increased by about 50 feet due to the influence of the plume. The plume samples collected by the copper tapes on all the three darts appeared to be reasonably clean. The cylindrical sleeves on the tethered darts were completely secured. The cylindrical sleeve mechanism was not activated on the third tethered dart due to breaking of the tether during the launch of the dart.

Results

Scanning Electron Microscope (SEM) analysis of the copper tapes from the different darts revealed a large collection of mostly spherical plume particles. Typical SEM micrographs of the samples from the MNASA tests and the FSM-4 test are shown in Figures 4a and 4b. The majority of the particles had a smooth surface and appeared dark brown under an optical microscope. The diameter of the particles varied from submicron to 16 μm in the MNASA samples and from 1-40 μm in the FSM-4 samples. The size distribution for a given sample was determined by measuring individual

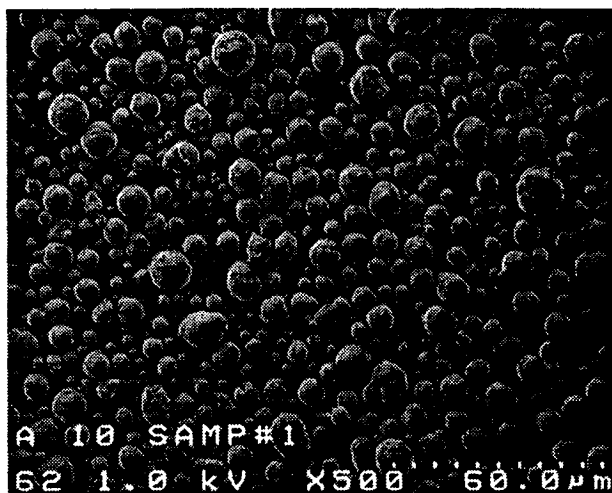


Figure 4a. Typical Plume Particles Sample from MNASA Tests

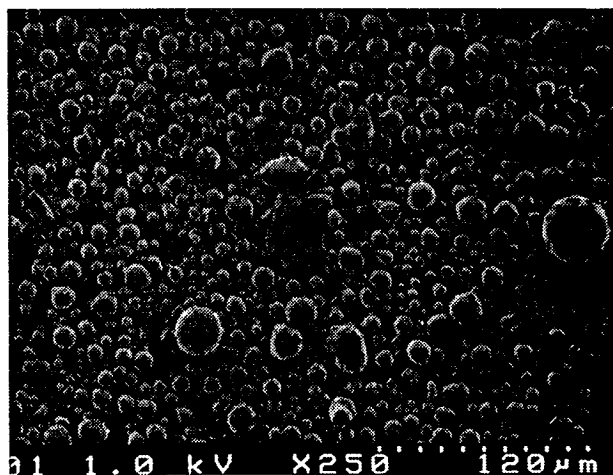


Figure 4b. Typical Plume Particles Sample from FSM-4 Test.

particles on enlarged SEM photographs using a scanner and a Macintosh personal computer.

Currently, the industry standard for calculating d_{43} for solid rocket motor Al_2O_3 plume particles at the nozzle exit plane is the Hermesen's correlation⁴ given by

$$d_{43} (\mu\text{m}) = 3.6304 D_t^{0.2932} [1.0 - \exp(-0.0008163 \xi_c P_c \tau)]$$

where D_t is the throat diameter in inches (Table 1 for the MNASA motors and 53.86 inch for the RSRM motor), ξ_c is the Al_2O_3 concentration inside the chamber in gm-mole/100 gm (0.262 for the RSRM propellant and 0.3 for the ASRM propellant), P_c is the chamber pressure in psia (Table 1 for the MNASA motors; about 880 psi at 12.3 seconds and about 630 psi at 68.3 seconds for the FSM-4 motor) and τ is the average residence time in the chamber in msec (estimated to be about 120 msec for the MNASA motor and 350 msec for the RSRM motor).

The measured mass averaged diameter, d_{43} , for a collected sample is determined from

$$d_{43} = \Sigma d_i^4 / \Sigma d_i^3$$

where the summation is carried over all the particles in the sample. All measured particle sizes in this report are at room temperature.

MNASA Motors

In all of the MNASA samples examined, the number of particles in each sample exceeded 1000. The mass distribution of these particles is shown in Figures 5-8. In a given sample, all particles under 2 μm were grouped into one size with a mean size of 1 μm . In all MNASA samples examined, nearly 80% of the particles measured were under 4 μm , but the mass-median diameter was always between 7.5 and 9.0 μm .

The measured d_{43} from each of the MNASA samples analyzed are compared in Table 2 to the value calculated from Hermesen's correlation. The measured d_{43} is always 10 to 30% higher than the calculated value but within the standard deviation of the correlation, $\sigma=0.298$ (corresponding to a deviation in d_{43} of about $\pm 35\%$)

Sample/Test	Measured	Hermesen	% Diff
D-1/S/MNASA 8	7.98	7.15	11.61
D-1/S/MNASA 9	8.57	7.17	19.53
D-1/1/4" T/MNASA 9	8.45	7.17	17.85
D-1/1/16" T/MNASA 9	8.19	7.17	14.23
D-2/1/4" T/MNASA 9	9.17	7.17	27.90
D-3/1/4" T/MNASA 9	8.69	7.17	21.20
D-4/1/4" T/MNASA 9	8.22	7.17	14.64
D-5/1/4" T/MNASA 9	9.21	7.17	28.45
D-1/S/ MNASA 10	8.86	7.18	23.40
D-1/1/4" T/MNASA 10	8.40	7.18	16.70
D-2/1/4" T/MNASA 10	8.89	7.18	23.82
D-3/1/4" T/MNASA 10	8.40	7.18	16.70

Table 2. Measured and Calculated Mass Averaged Diameter for the Samples of MNASA Plume Particles Analyzed. (S and T in the Table represent Shaft and Tube respectively).

Figure 5 shows the cumulative mass fraction plotted against the plume particle size for one of the samples analyzed. Also shown in the figure is the best fit of the data, a log-normal distribution with a standard deviation of 0.14. The size distribution of each MNASA sample analyzed was best curve fitted by a log-normal monomodal distribution with the standard deviation varying from 0.13 to 0.17.

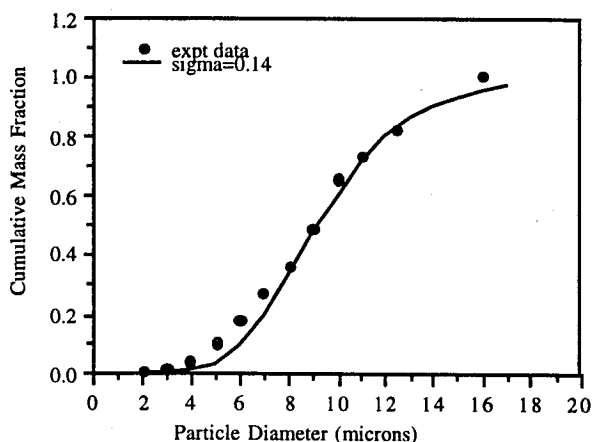


Figure 5. Cumulative Mass Fraction for Plume Particle Sample Collected by Dart 1 of MNASA 9 Test

In addition to the above general trends, the following features were observed:

(1) Figure 6 shows a comparison of the size distributions of the particles collected on the shaft of the projectile launched 1 second after motor ignition in MNASA 8-10 tests. The size distribution is not

significantly different among the different motors. Motors 9 and 10 were identical except for the propellant formulation. Furthermore, the variation in propellant formulation, including percentage aluminum, does not appear to affect the size distribution of Al_2O_3 particles in the plume. This result indicates that the plume particle size distribution is primarily dictated by the throat diameter.

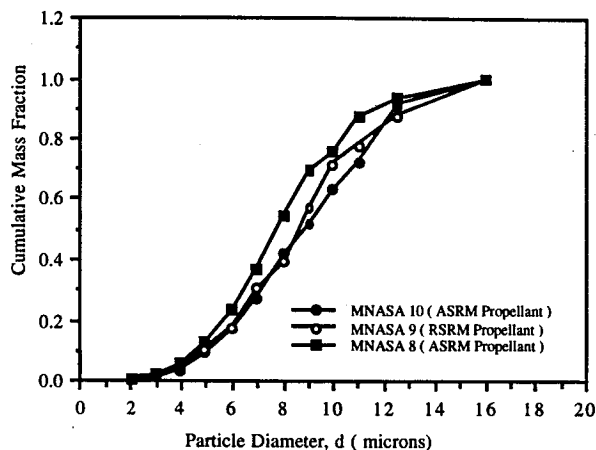


Figure 6. Comparison of Size Distribution of Plume Particle Samples Collected by the Shaft of Dart 1 in the Three MNASA Tests.

(2) Figure 7 shows a comparison of the size distribution of the particles collected by the 1/4-inch diameter wire on darts 1-5 from MNASA 9 test. The distribution is not significantly different among samples from different projectiles indicating absence of any variation in plume particle size distribution with motor burn time.

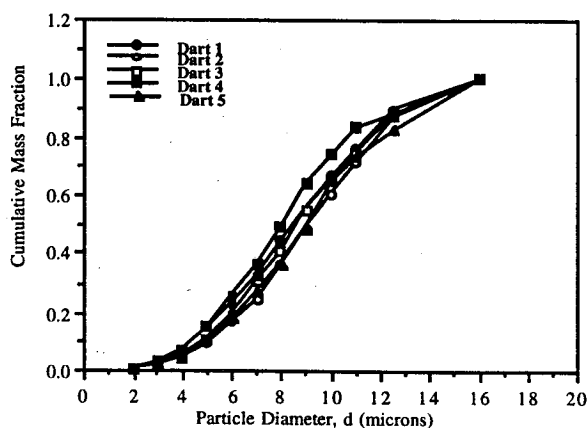


Figure 7. Comparison of Size Distribution of the Plume Particles Collected by the 1/4-inch at Different Burn Times in MNASA 9 Test.

(3) There is an unknown bias in the determination of the size distribution of the particles collected on the projectile shaft due to its large diameter. Small particles (typically $< 4 \mu\text{m}$) may tend to follow the flow around the projectile and may not impinge on it. Consequently, the particles collected by the 1.5-inch diameter shaft may be biased toward the large particles. However, the relative velocity between the projectile and the plume gas will tend to reduce this bias. Figure 8 shows a comparison of the size distribution of the particles collected on the shaft and the 1/4-inch and 1/16-inch diameter wires from the projectile in MNASA 9 test. Though the finer wires indicate slightly higher mass fractions of smaller particles, as expected, the distributions do not appear to be significantly different. Nearly 80% of the particles collected by the shaft were under $4 \mu\text{m}$, indicating that the bias in the size distribution of the particles collected by the shaft of the projectiles is negligible.

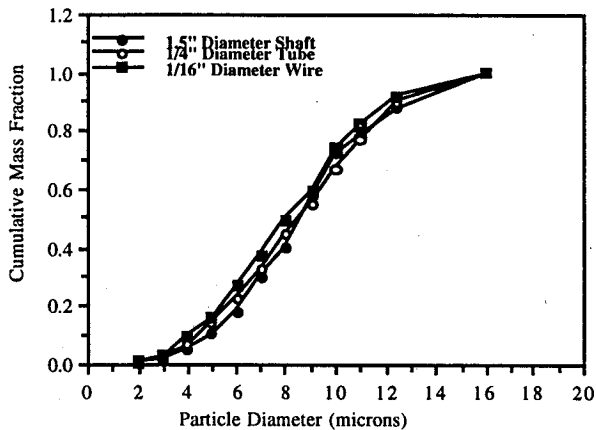


Figure 8. Comparison of Size Distribution of the Plume Particles Collected on Different Surfaces of Dart 1 in MNASA 9 Test.

To assure that the diameter of the spherical particles measured from the MNASA tests were that of the plume particles primarily containing aluminum oxide, the composition of the particles was determined from the wave length dispersive spectrum of individual particles. This was done using an electron microprobe on randomly selected particles and is illustrated in Figure 9. Moreover, the optical properties of the Al_2O_3 plume particles (both solid and molten) are functions of the contaminants in them¹². The contaminants included Ag, Fe, Cu, Cr, Ca, Ni, Si, Sn, Mg, and Mn and their individual levels were under 1% by weight. The accuracy of the contaminant level is questionable due to the spherical nature of the particles analyzed. The electron beam tends to scatter at different

angles and may not be fully captured by the sensor elements in the microprobe. Similar contaminant measurements have been made by AEDC on the plume particles collected from IUS-2, PAM D-II motors¹³ using spark spectroscopy. These analyses indicated contamination levels in the 1 to 3% range, higher than what were measured in the MNASA plume particles.

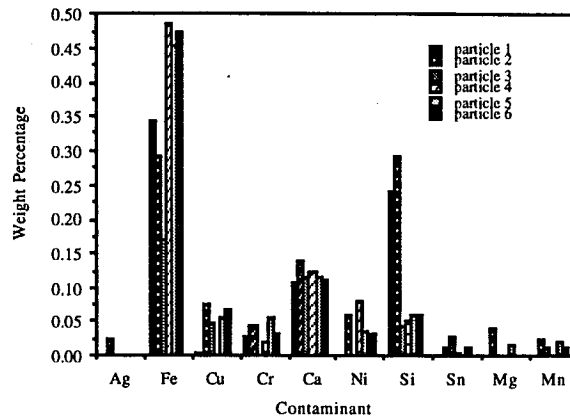


Figure 9. Electron Microprobe Analysis of a few MNASA 8 Plume Particles Using Wave Length Dispersive Spectrum.

Spark spectroscopy is a more accurate method for predicting the contaminant levels in the plume particles. However, a 50-mg sample would be required to perform such analysis and the collection method employed here was not adequate to collect such large samples.

FSM-4 RSRM Motor

The results from the four darts in the FSM-4 test are summarized in Table 3. The particles collected by dart 4 appeared similar to those collected by darts 1 and 3 and consequently a distribution was not measured from the dart 4 samples.

Dart #	Burn Time	No. of Particles Analyzed	d_{43} (contaminated)	d_{43} (clean)
1	12.3	3700	13.74	11.2
2	67.0	0*	-	-
3	68.3	4040	11.58	10.97
4	93.5	0	-	-

* contaminated sample due to sleeve malfunction.

Table 3. Summary of Results from the Four Darts Launched Through the Plume in FSM-4.

In FSM-4 sample analysis, dimensions of particles over 3 microns were obtained from SEM micrographs of sample areas magnified at 250x. Dimensions of particles under 3 microns were obtained from smaller areas within the same sample area magnified at 500x. To determine the particle size distribution, the number of particles from the 500x magnifications were multiplied by four and added to the number of particles from the 250x magnification. Since the Al_2O_3 plume particles are expected to be spherical due to the surface tension forces in the liquid phase droplets during their traverse through the nozzle, any non-spherical particles collected on the tape was not included in the size distribution analysis. Spherical particles stuck together were included and each particle in the cluster was measured individually. The Hermesen correlation d_{43} for the FSM-4 conditions was calculated to be $11.68 \mu m$ and is primarily dictated by the throat diameter.

Figure 10 shows the cumulative mass plotted against the particle diameter for the plume particle sample collected by the tethered dart launched at 12.3 seconds after motor ignition. A total of 3700 particles were measured to obtain this distribution. These spherical particles were obtained from two SEM micrographs of random locations on two different tapes from the same dart. Only five particles among these 3700 were above $23 \mu m$. For this sample, the test derived d_{43} was determined to be $13.74 \mu m$.

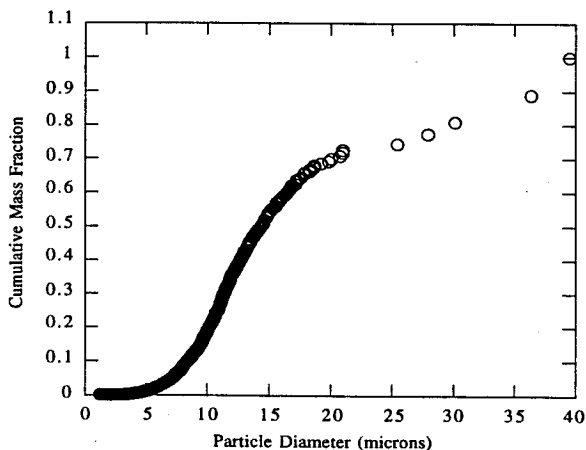


Figure 10. Cumulative Mass Fraction of 3700 Plume Particles Measured from Dart 1 of FSM-4. Dart 1 was Launched at $t=12.3$ seconds after Motor Ignition.

Figure 11 shows the cumulative mass plotted against the particle diameter for the plume sample collected by the control dart launched at 68.3 seconds after motor ignition. The chamber pressure of the

motor is about 630 psi at this time frame. A total of 4040 particles were measured to obtain this distribution and these particles were obtained in the same manner as described above. Only two particles among these 4040 were above $23 \mu m$. The test derived mean mass averaged diameter, d_{43} , was determined to be $11.58 \mu m$.

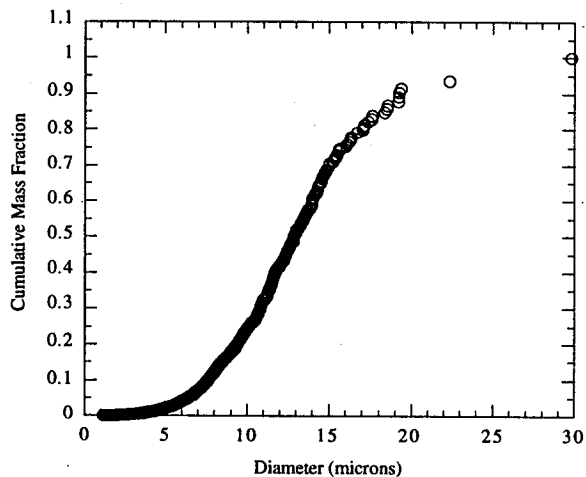


Figure 11. Cumulative Mass Fraction of 4040 Plume Particles Measured from Dart 3 of FSM-4. Dart 3 was Launched at $t=68.3$ seconds after Motor Ignition.

As described before, the composition of the plume particles was determined from the wave length dispersive spectrum of the individual particles using an electron microprobe. These plume particles were chosen randomly from samples from the two darts. A total of 26 particles were analyzed varying in diameter from $5 \mu m$ to $40 \mu m$. The results of the analysis are illustrated in Figure 12. The results clearly indicate that the plume particles in the $23 - 40 \mu m$ range were heavily contaminated with calcium and silicon from the ground. These contaminants were not restricted to the surface of the particles. Therefore, these large particles were assumed to be a result of the plume/ground interaction and were removed from the data set. Particles below this size range were primarily aluminum oxide particles.

Figure 13 shows a reformulation of the cumulative mass distribution for the plume particle sample collected by the tethered dart launched at 12.3 seconds after motor ignition. In this plot, all particles $23 \mu m$ and above were deleted due to the results of the electron microprobe analysis. The test derived mass averaged diameter, d_{43} , is reduced from $13.74 \mu m$ to $11.2 \mu m$. Also shown in this figure is the best fit of the data; a monomodal log-normal distribution with a standard deviation of 0.13. Figure 14 shows a similar plot for

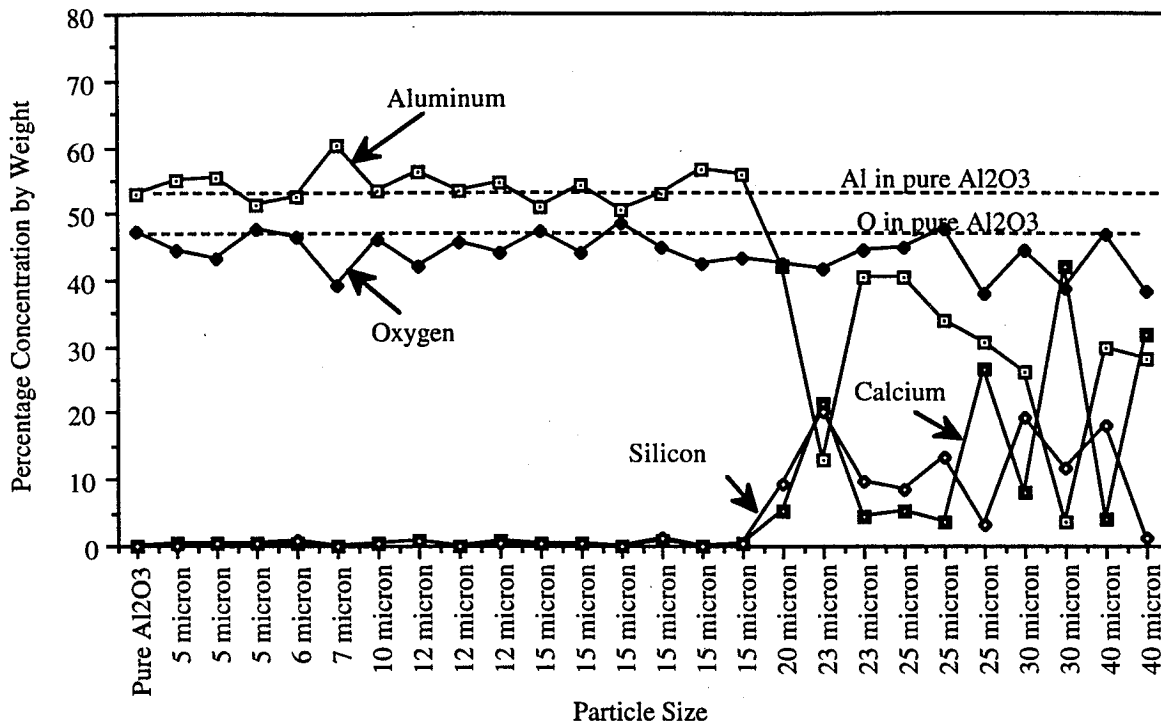


Figure 12. Composition of Discrete Plume Particles Analyzed from Wave Length Dispersive Spectrums Using An Electron Microprobe.

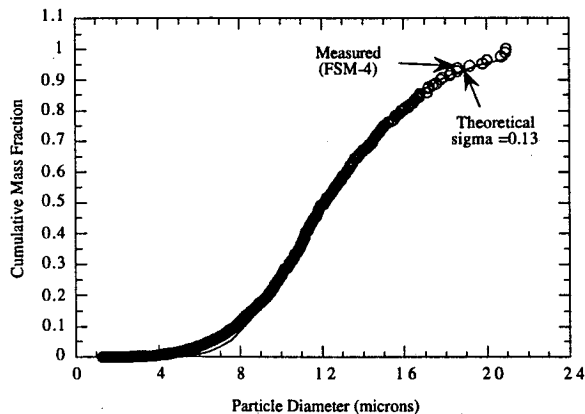


Figure 13. Cumulative Mass Fraction of all Plume Particles Below 23 μm Measured from Dart 1. The Best Fit of the Measured Data is Given By A Log-normal Curve with a Standard Deviation of 0.13.

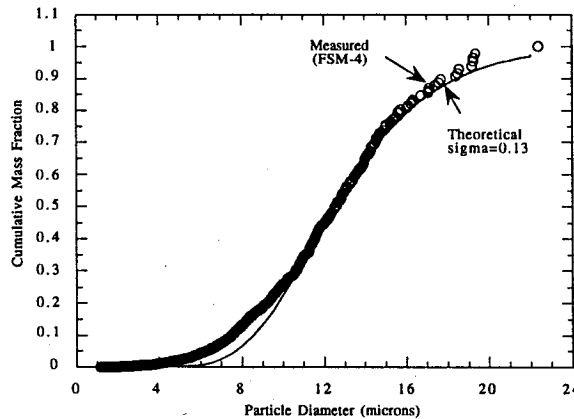


Figure 14. Cumulative Mass Fraction of all Plume Particles Below 23 μm Measured from Dart 3. The Best Fit of the Measured Data is Given By A Log-normal Curve with a Standard Deviation of 0.13.

the sample collected by the control dart launched at 68.3 seconds. The mass averaged diameter is reduced to 10.97 μm and the best curve fit is again described by a monomodal log-normal distribution with a standard deviation of 0.13. These distributions agree extremely well with that predicted by Salita⁶ at the exit plane of the full-scale RSRM using the OD3P code.

The mass averaged diameter measured from the FSM-4 plume particle samples were smaller compared to the 11.68 μm calculated using Hermsen's correlation and the 13.2 μm (after correction to room temperature) predicted by Salita⁶ at the nozzle exit plane. This could be due to the fact that these samples were collected 300 feet aft of the nozzle exit plane where the few largest particles might have already precipitated out. Another possible reason could be the omission of particles above 23 μm , since these omitted particles could have contributed to the mass fraction of the larger particles if they were not contaminated. However, the measured mass averaged diameter of the FSM-4 plume particle samples is well within the standard deviation of the Hermsen's model, $\sigma=0.298$ (corresponding to a deviation in d_{43} of about $\pm 35\%$).

Conclusions

It has been demonstrated that the dart system developed for the MNASA program can be adapted for collecting reasonably clean Al_2O_3 plume particle samples from static firings of the full-scale RSRM motor. This is the first time that clean plume particle samples have been obtained during the static firing of the RSRM motor. The mass averaged diameter, d_{43} , measured from these samples agree with that calculated using the industry standard Hermsen's correlation within the standard deviation of the correlation. The measured cumulative mass fraction of the aluminum oxide plume particles plotted as a function of the particle diameter measured from these samples agreed well with the theoretically predicted distribution by Salita at the exit plane of the RSRM nozzle and was best represented by a monomodal log-normal distribution with a standard deviation of 0.13.

Acknowledgment

The author expresses his sincere appreciation to Jim Taylor, Ray Kirch, W.B. Clifton, Steve Allums, Chuck Vibbart, Joe Garner, Steve Cato, Greg Jerman, the Hot Gas Facility personnel of Martin Marietta at Huntsville, Alabama, the RSRM Chief Engineer's

office at the NASA/Marshall Space Flight Center, and the Thiokol Corporation Space Operations at Wasatch, Utah for their assistance and cooperation during this project. This project would not have been successful without the innovative ideas of the people mentioned above. The author sincerely appreciated the upbeat attitude of Ray Kirch and W.B. Clifton in spite of the initial technical difficulties in our efforts to collect plume particles from the RSRM.

Reference

- [1] Reardon, J.E., "Rocket Plume Base Heat Transfer Methodology," AIAA 93-2823, AIAA 28th Thermophysics Conference, July 1993.
- [2] Nelson, H.F., "Backward Monte Carlo Modeling for Rocket Plume Base Heating," Journal of Thermophysics and Heat Transfer, Volume 6, No.3, July 1992.
- [3] Smith, S.D., "High Altitude Chemically Reacting Gas Particle Mixtures Volume III - Computer Code User's and Application Manual," LMSC-HREC TR D867400, October 1984.
- [4] Hermsen, R.W., "Aluminum Oxide Particle Size for Solid Rocket Motor Performance Prediction," Journal of Spacecraft and Rockets, Volume 18, No.6, November 1981.
- [5] Salita, M., "Survey of Recent Al_2O_3 Droplet Size Data in Solid Rocket Chambers, Nozzles, and Plumes," Presented at the JANNAF 1994 Joint Meetings 31st Combustion Subcommittee, 17-21 October 1994.
- [6] Salita, M., "Implementation and Validation of the One Dimensional Gas/Particle Flow Code OD3P," CPIA Pub 498, pp 69-81, 25th JANNAF Combustion Meeting, October 1988.
- [7] Girata, P.T., McGregor, W.K., Quinn, R., "Inertial Upper Stage Solid Rocket Motor Core Flow Sampling at Higher Altitudes," AEDC-TR-83-1, November 1983.
- [8] Strand, L.D., Bowyer, J.M., Varsi, G., Laue, E.G. and Gauldin, R., "Characterization of the Exhaust Particulates in the Ground Cloud and High Altitude Plume of Large Solid Propellant Booster Rockets," AIAA-80-0354, AIAA 18th Aerospace Sciences Meeting, January 1980.

[9] Kohlbeck, J.A., Elmslie, J.S., Wolf, S.D and Mitchell, E.M., "Al₂O₃ Collection from Exhaust Plumes of Full-scale Motor Tests," 25th JANNAF Meeting, Volume III, CPIA Publication No. 498, October 1988.

[10] Laredo, D., McCrorie, J.D., Vaughn, J.K., and Netzer, D.W., "Motor and Plume Particle Size Measurements in Solid Propellant Micromotors," Journal of Propulsion and Power, Vol.10, No.3, pp 410-418, May-June 1994.

[11] Gomes, P.V., et al., "Nozzle Geometry and Additive Effects on Plume Particulate Behavior in

Subscale Solid Propellant Rocket Motors," CPIA Pub. 621, Volume II, October 1994.

[12] Konopka, W.L., Reed, R.A., and Calia, V.S., "Measurements of Infrared Optical Properties of Al₂O₃ Rocket Particles," Progress in Astronautics and Aeronautics, Volume 91, 1984.

[13] Calia, V.S., Celentano, A., Soel, M., et al., "Measurements of UV/VIS/LWIR Optical Properties of Al₂O₃ Particles," 18th JANNAF Meeting, November 1989.